# INVESTIGATION OF THE ROOT CAUSE OF FLOW DIPS AT PICKERING B

by
H.W. Hinds
Atomic Energy of Canada Ltd.
Chalk River, ONT

## ABSTRACT

Pickering Nuclear Generating Station (PNGS) B has recently raised its flow trip-point and is now experiencing a number of low-flow alarms. These alarms are caused by "flow dips" which are very short but fairly large drops in measured differential pressure (DP) across the flow-measuring orifice plates. Similar flow dips have been reported at other CANDU®[1] stations. The purpose of this present study is to determine the root cause of these flow dips.

A set of high-bandwidth pressure and accelerometer measurements were made at PNGS unit 7. The data shows that the high and low sides of the DP cell do receive large (>100 kPa) pressure pulses and exhibit lightly damped resonant responses, except that the resonant response of the low-side impulse line becomes heavily damped after the second cycle, coincident with a build-up of high-frequency mechanical motion, especially in the low-side impulse line. Several possible theories to explain the cause of flow dips are given.

On an operating reactor such as PNGS B, it is recommended that the flow transmitters be changed to the adjustable-damping type, and that their time constants be increased. This should be acceptable to safety and licensing, since the current DP cell time constant is much shorter than the licensing requirement. Recommendations are made on how to avoid similar flow dip problems in new plants.

## 1. INTRODUCTION

The primary heat transport (PHT) system for a CANDU reactor consists of four quadrants, each fed from its own inlet header through a large number of inlet feeders. Part of the SDS1 safety system for a CANDU reactor is a measurement of reactor coolant flow. The flows in three inlet feeders per quadrant are monitored using orifice plates, impulse lines and differential pressure (DP) transmitters. If one of these three measurements indicates low flow (i.e., below the trip point), a low gross flow (LGF) alarm occurs; if two out of three measurements on the same quadrant indicate low flow, a reactor trip occurs on LGF.

As part of the movement to tighter safety margins, Pickering Nuclear Generating Station (PNGS) B raised its LGF trip point from 84% of nominal flow to 90%. As a result of this tighter margin, PNGS B began experiencing a number of LGF alarms, up to 30 per day. The output of four DP

---

[1] CANDU® is a registered trademark of Atomic Energy of Canada Limited (AECL).

transmitters is shown in Figure 1 [1]. These alarms are caused by the very short (70 ms) but fairly large (up to 22%) drops in measured DP as is evident in the second and fourth traces. This short deep drop in DP is termed a flow dip. If these "flow dips" were a true interruption of flow (and as discussed below, they are not), a 22% drop in DP translates to an 12% drop in flow [2].

An initial investigation determined that flow dips are not correlated to any other measured signal, including the corresponding inlet header pressure or the flow in other monitored channels (i.e., the FINCH channels) fed from the same header [1]. The conclusion of this first study was that the flow dips were a local turbulence phenomena related to orifice plates, and they were not caused by low flow in the quadrant as a whole or in the individual channel.

Flow dips can be easily filtered out by increasing the damping (time constant) of the DP transmitters. The manufacturer's specified time constant is 200 ms. The time constant of the total measurement loop in the Safety Analysis Report [3] is 350 ms, of which 200 ms is assigned to the transmitter and 150 ms is assigned to the alarm unit. The safety case has been reanalyzed and it was found that a 550 ms time constant for the transmitter is acceptable. The Atomic Energy Control Board (AECB) allowed PNGS B to increase the time constant up to 550 ms, maximum, on the one particular transmitter (unit 6 F4D) that was causing the most problems, but at the same time requested that PNGS B discover the root cause of the flow dip phenomena [4]. The purpose of this investigation is to determine this root cause. Following this study, the AECB is expected to allow a more generalized increase in time constants up to 550 ms, maximum, as required. This would eliminate all operational problems associated with flow dips.

It is also noted that similar flow dip problems have occurred at both Bruce [5] and Darlington [6]. It appears that flow dips are a generic phenomena with CANDU stations; whether they cause operating problems depends on the details at each station, and in particular, the setting of the LGF trip point.

The present report describes the recent set of measurements at PNGS and the results of their analyses. Conclusions and recommendations for existing and new plants are provided.

## 2. GENERAL DATA AND OBSERVATIONS

The LGF measurements at PNGS B are made across orifice plates in 1.925 inch feeder pipes; the diameter ratio for the orifice plates is 0.75. The orifice plates has D and D/2 taps. The manufacture and installation mostly conforms to the ISO Standard 5167[2] [2], with the following exceptions:

- the actual thickness of the orifice plate is 3/16 (0.1875) inch, whereas the standard (clause 7.1.4.3) specifies a maximum thickness of 0.09625 inch (0.05 D),
- the actual diameter of the pressure taps is 0.190 inch, whereas the standard (clause 7.2.1.4) specifies a maximum diameter of 0.146 inch (0.08 D), and
- the tappings are at 40° to the previous pipe bend, whereas the standard (clause 6.2.7) recommends that they be perpendicular to the plane of the bend.

[2] It is not surprising that the orifice plates do not exactly conform to the standard, as the design occurred in 1975-76, prior to issuance of the standard in 1984.

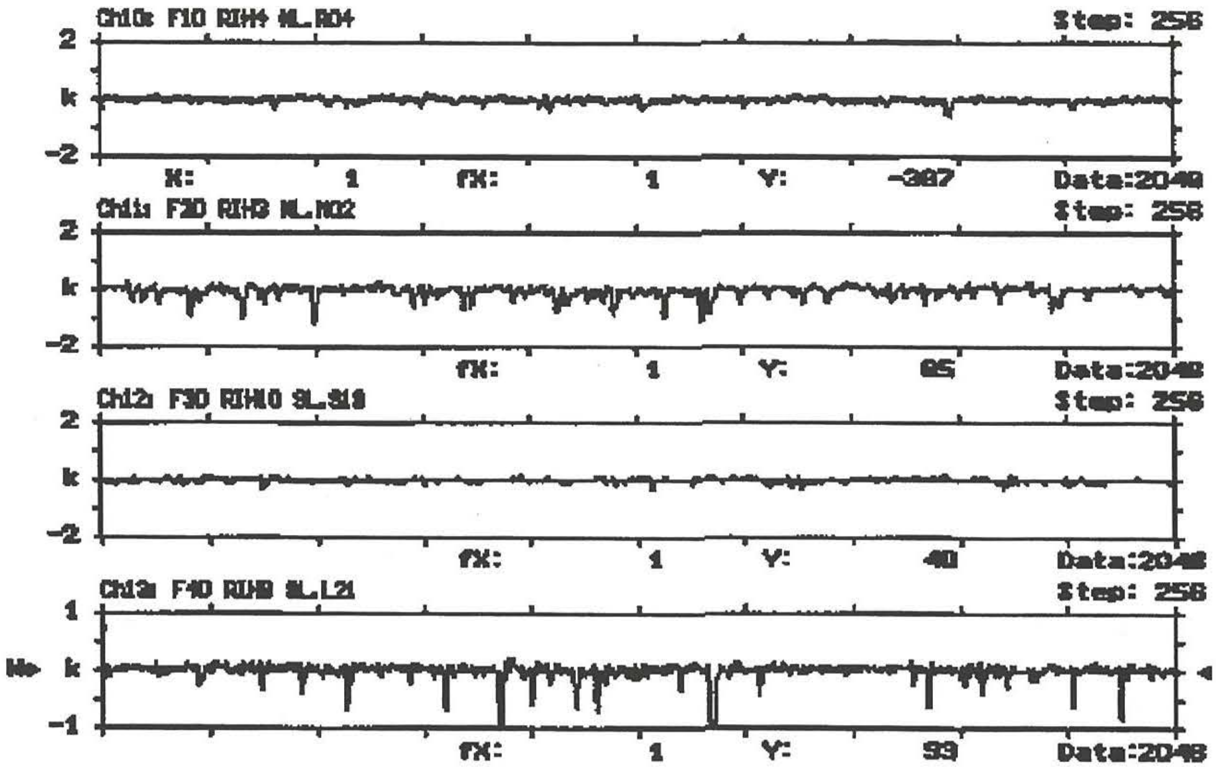

Figure 1 [1, Fig 2.3]: DP transmitter output as a function of time for four DP transmitters in PNGS unit 6. The bottom of each trace is approximately the alarm point. The time axis is 0 to 20.48 s. Flow dips are clearly evident in the second and fourth traces. Two of the flow dips in the fourth trace might have caused low gross flow alarms.

Also, there are only 24 diameters of straight pipe upstream of the orifice, which implies an additional 0.5% uncertainty in the calibration accuracy.

The impulse lines, also called "instrument sensing lines", are nominal 3/8 inch tubing (7.04 mm ID) about 30 to 45 m long, depending on the distance and routing from the tap locations to the DP instrument (Figure 2). There is a 3-valve manifold for isolating and balancing each transmitter. There is a Hoke valve for isolating the high side, and a second Hoke valve and a pair of manual needle valves for equalizing the transmitter; these are used during safety-system process-trip tests. The transducers are all (except that on unit 6 F4D) Rosemount Model 1152 with range up to 690 kPa and fixed damping (nominally 200 ms). The transmitter on unit 6 F4D was recently changed to a similar model, but with adjustable damping; the time constant was increased to 500 ms nominal.

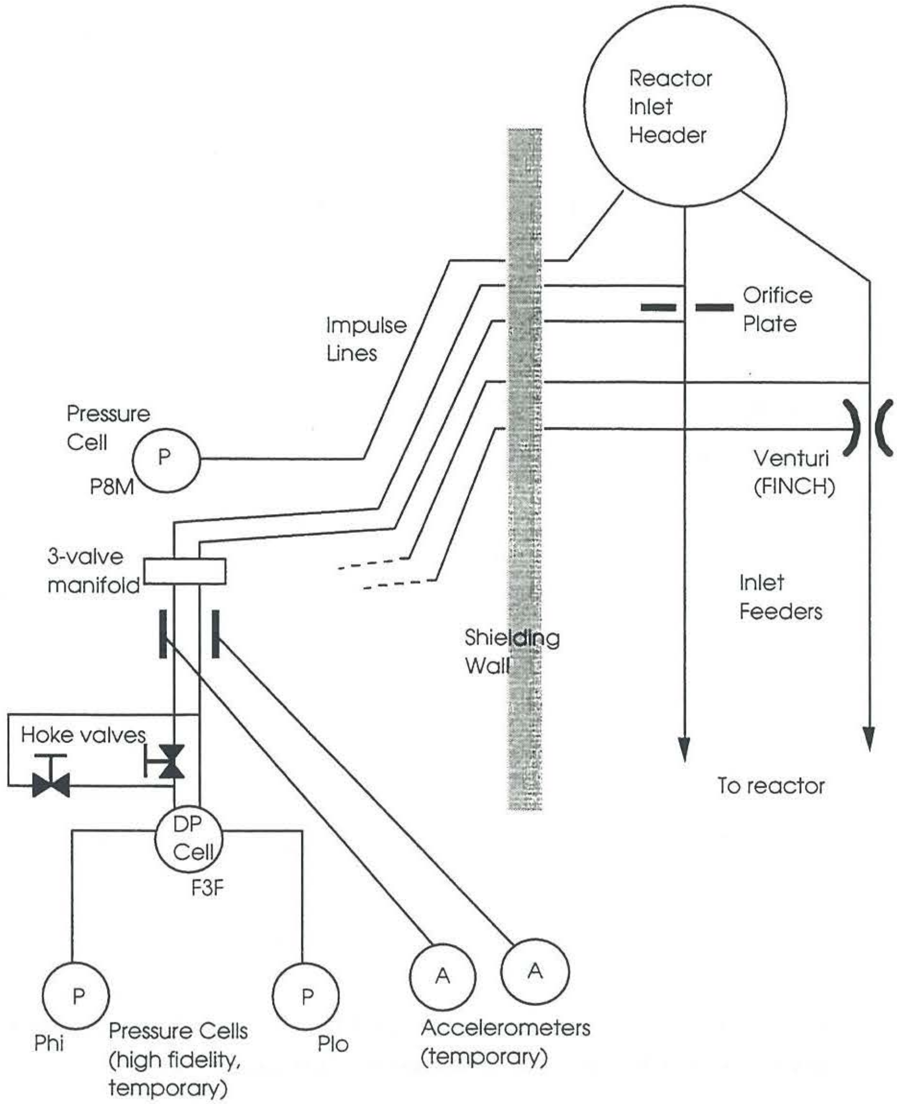


Figure 2: Simplified schematic of a typical DP cell arrangement also showing the location of temporarily-installed pressure cells and accelerometers.

Before increasing the time constant, the transmitter causing the greatest number of alarms in PNGS B was F4D unit 6, which is on inlet feeder L21. The nominal flow in this feeder is 18.37 kg/s [7], which leads to a DP of 310 kPa at the DP cell [8] and a total pressure drop after recovery of 128 kPa [2]. The transmitter is calibrated to 470 kPa full scale, which represents 120% of nominal flow. A flow dip of 10% in flow corresponds to a pressure change of approximately 60 kPa.

Since adjusting the damping on unit 6 F4D, the transmitter causing the greatest number of alarms at PNGS B is F3F in unit 7, which is on inlet feeder M21. The nominal flow and other hydraulic parameters of this feeder are similar to that of F4D unit 6. The transmitter is calibrated to 491 kPa full scale.

Flow dips occur on all SDS1 LGF measurements, all of which are on 1.925 inch feeders, and use orifice plates, but the amplitude and approximate frequency of occurrence varies considerably (Figure 1). No flow dips occur on the Reactor Regulating System (RRS) fully instrumented channel (FINCH) flow measurements, which are on 2.478 and 2.920 inch feeders, and which use venturis as the primary elements. The FINCH measurements also have no Hoke or needle valves, as they do not undergo process-trip tests.

It is possible to feel mechanical vibration from both general "noise" and sharp "hits" in all the impulse lines leading to all the SDS1 LGF transmitters. Some of these impulse lines are also visibly vibrating with an amplitude of up to 3/8 inch in the area between the vault wall and the transmitter rack. No such noise, hits or vibration is evident on any other impulse line, including those for the FINCH channels.

Operating experience has shown that the characteristics of the flow dips can be modified by changing primary coolant pump configuration. (PNGS has a system that uses three out of four pumps per quadrant.) When the pump feeding the header turret nearest to the feeder being monitored is ON, the flow through that feeder increases a few percent. The flow noise increases as the number and frequency of medium-sized dips increases. However, the number of large dips decreases, thereby decreasing the LGF alarm frequency. A study into the effects of changing pump arrangement has been completed [9].

## 3. DARLINGTON EXPERIENCE

At Darlington, similar flow dip problems were experienced during early operation, and an investigation was launched [6]. However, before results were obtained, the pressure-tube-fuel-bundle-fretting problem appeared, and effort was redirected to investigate its cause. An extensive experimental program was initiated to measure pressures at numerous locations around the coolant loop, as well as other variables, such as bundle motion.

These measurements and their analysis eventually identified acoustic resonance at the pump vane passing frequency as the source of the pressure-tube-fuel-bundle-fretting problem, and led to a change from 5-vane to 7-vane impellers in the PHT pumps. This change also caused a change in the frequency of occurrence of the flow dips [10]. However, the theory that the flow dips might be indicative of actual flow changes which were causing the fuel damage had already been ruled out. Consequently, interest in finding the root cause of flow dips waned, but several interesting measurements and analytical studies were completed [6, 10, 11 and 12].

In particular, large pressure dips (and also some pressure peaks) at certain locations in the inlet headers were found (Figure 3). The dips were considerably larger (>120 kPa) near the inlet turrets than at other locations; the pressure noise at other locations in the inlet headers was found to be generally less than 50 kPa peak. Thus, there are large pressure dips at certain locations in the inlet headers that do not occur at other locations, even within the same header. Randomly-spaced pressure pulses (e.g., 120 kPa amplitude) were also found to be travelling down feeder R13 at acoustic velocity; these pressure pulses start with a negative-going cycle.

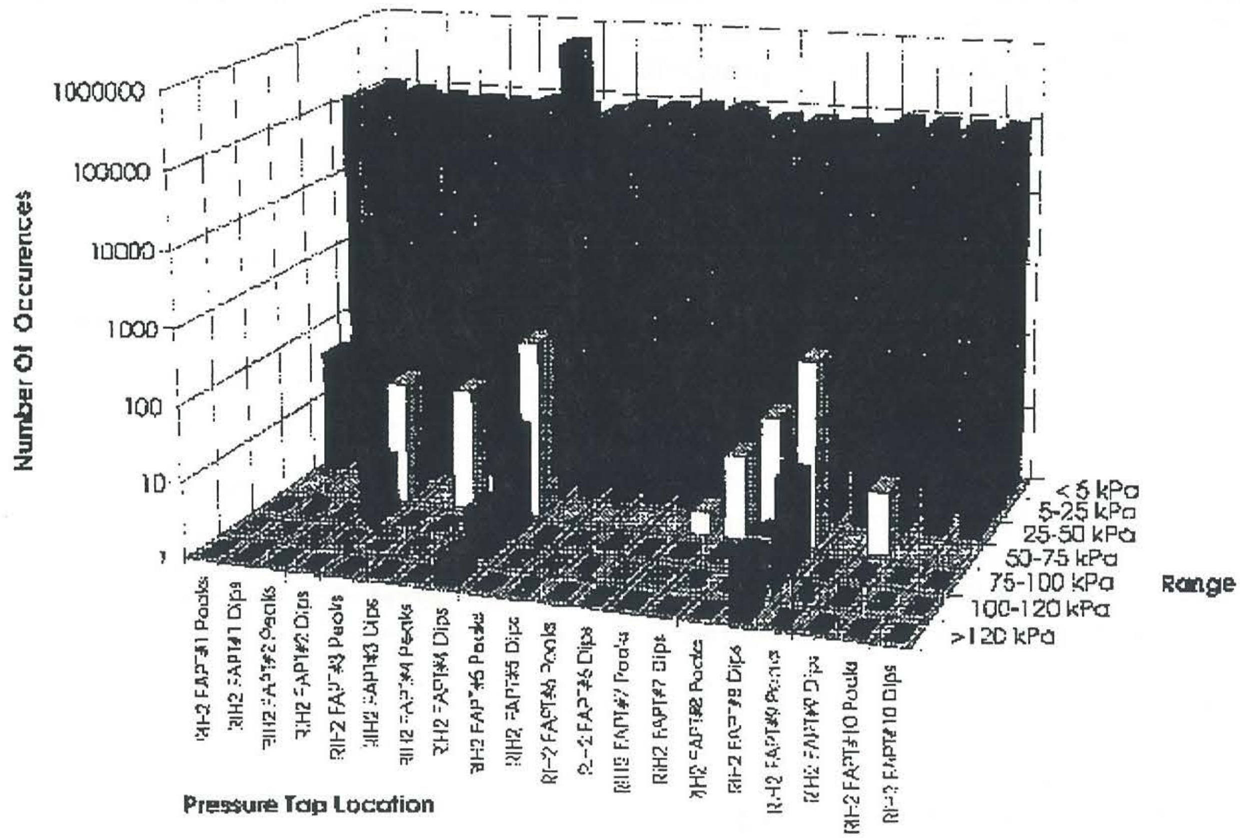


Figure 3 [11, Fig 2.2.2]: Histogram of pressure peaks and dips in a 400 second sample as a function of peak/dip amplitude and location along the header

## 4. MEASUREMENTS AT PNGS

### 4.1 Setup

In 1995 March, on PNGS unit 7, measurements, using both permanent PNGS instruments and temporary pressure cells and accelerometers, were made of the following variables:

(1) SDS1 DP (F3F-FT1)
(2) FINCH DP (F1C-FT7)
(3) Pressure on the high side of F3F transmitter (Phi) (high fidelity)
(4) Pressure on the low side of F3F transmitter (Plo) (high fidelity)
(5) Pressure on the high side of the FINCH channel transmitter (high fidelity)
(6) Pressure on the low side of the FINCH channel transmitter (high fidelity)
(7) ECI pressure in RIH (P8M-PT1)
(8) SDS1 pressure in ROH (P3F-PT1)
(9) x-axis accelerometer in high leg of F3F transmitter (Xhi)
(10) z-axis accelerometer in high leg of F3F transmitter (Zhi)

(11) x-axis accelerometer in low leg of F3F transmitter (Xlo)
(12) z-axis accelerometer in low leg of F3F transmitter (Zlo)
(13) x-axis accelerometer in high leg of FINCH transmitter
(14) z-axis accelerometer in high leg of FINCH transmitter
(15) x-axis accelerometer in low leg of FINCH transmitter
(16) z-axis accelerometer in low leg of FINCH transmitter

The F3F DP, the FINCH DP and the pressures in the RIH and ROH (variables 1, 2, 7 and 8) are permanent PNGS instruments, having relatively low bandwidth.

The pressures on the two sides of the F3F and FINCH transmitters (variables 3 through 6) were measured with temporary high-bandwidth piezoelectric sensors, which can withstand high static pressure while having high sensitivity to small pressure changes. They operate as a band-pass filter, with both a low-frequency breakpoint (50 s time constant) and a high-frequency limit (>100 kHz). They were installed using about 250 mm of tubing to the drain holes of the DP cells (Figure 2).

The accelerometers (variables 9 through 16) were temporarily installed by Ontario Hydro Research on the impulse lines a few feet from the DP cells (Figure 2).

The signals were measured concurrently using two data acquisition systems:

1) a noise analysis data acquisition system, used in previous tests (e.g., [1]). Noise data was collected, with high resolution, with sampling frequencies of 300, 100 and 50 Hz in three tests. Anti-aliasing filters matched to the sampling frequency were used.
2) a LabView data acquisition system with 16-bit resolution, and up to 3000 Hz sampling. A set of 1 kHz bandwidth isolation amplifiers acted as crude anti-aliasing filters.

## 4.2 Data Analysis

The basic data analysis was performed by Ontario Hydro on the data collected with the noise analysis system using the noise analysis software. Similar analysis was performed by Chalk River Labs on the data collected on the LabView data acquisition system using the MATLAB analysis package. The results of these two separate analyses are similar; only the latter is described here.

### 4.2.1 Mathematical Treatment of Signals

The pressure signals collected using the LabView system were first converted into pressure units (kPa), so that they could be directly compared. The difference between the high-side pressure (Phi) and the low-side pressure (Plo) was also calculated:

$$\text{Diff} = \text{Phi} - \text{Plo} \tag{1}$$

Because Phi and Plo are both high-fidelity measurements, the value of Diff is taken as a true measure of the differential pressure across the DP cell. Due to the bandpass filtering inherent in the high-fidelity pressure transducers, the dc value of Diff is arbitrary.

To better visualize what is happening with the accelerometer signals during a flow dip, the accelerometer signals were divided into two bands by filtering with phaseless fourth-order Chebychev band-pass filters:

| | |
|---|---|
| mid-frequency: | 50 - 250 Hz |
| high frequency: | above 250 Hz |

The original accelerometer signal and each of the bands individually were processed to extract the envelopes of the high-/mid-frequency noise. The envelope signals are labelled FiltXlo, FiltZlo, FiltXhi, and FiltZhi.

The results given here are all from a run collected using the LabView system with 2200 Hz sampling.

### 4.2.3 Standard Analysis

Standard analysis of the signals is based on simple time histories, power spectral densities, transfer functions and coherence functions, all performed on all the data divided into blocks.

Figure 4 shows plots of several key variables on an expanded scale about a typical flow dip. The dip in the output of F3F, the standard PNGS B DP cell, is about -50 kPa (Figure 4a). The corresponding Diff signal has a minimum of about -250 kPa, which implies that the actual pressure difference across the DP cell is nearly zero (Figure 4d). The largest dip discovered to date was -500 kPa in Diff, which implies that the pressure difference across the DP cell was actually significantly negative (i.e., reversed from normal). The dip in the output of F3F (Figure 4a) occurs somewhat later than the corresponding dip in Diff (Figure 4d); in fact, the two signals appear to be almost out of phase. These features are both due to the low-pass filtering action of the F3F transmitter. The Phi and Plo signals from the temporary high-fidelity pressure cells both show a lot of noise, up to 800 kPa peak-to-peak (Figures 4b and 4c). The patterns for the accelerometer signals Xhi and Zhi, which are practically identical to each other, do not exhibit any consistently obvious features near the flow dips, while those for Xlo and Zlo, which are also practically identical to each other, appear to have a burst of activity at about the same time as the flow dips (Figure 4e); this mechanical motion activity has been shown to be of high frequency (>250 Hz).

Power spectral densities (PSDs) were found for each signal and those for Phi and Plo are shown in Figure 5 over the first 50 Hz. There are large peaks at 10, 30, 50 Hz, etc. in all pressure signals. These expected peaks are due to the hydraulic-acoustic resonances of the impulse lines based on the their lengths and the velocity of sound in water. The small dip in the Plo PSD at 6 Hz was not expected; it is a consequence of the Plo/Phi transfer function discussed below.

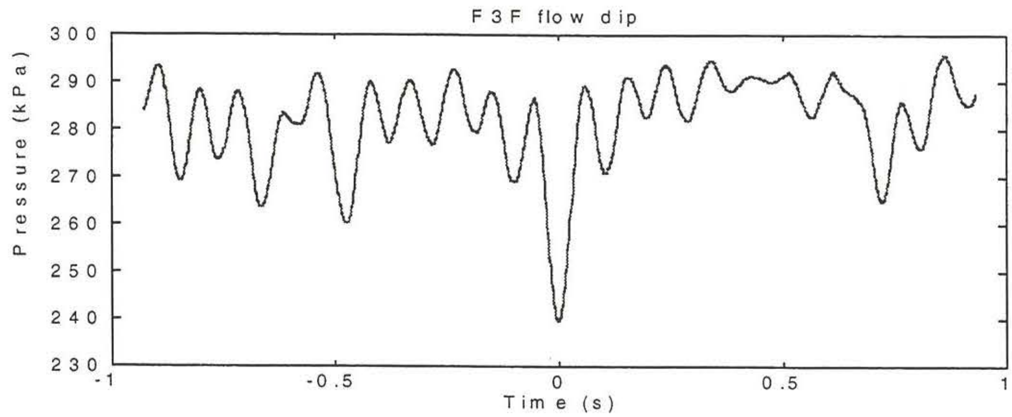


Figure 4a: Plot of F3F, the output of the standard PNGS B DP cell, near a flow dip.

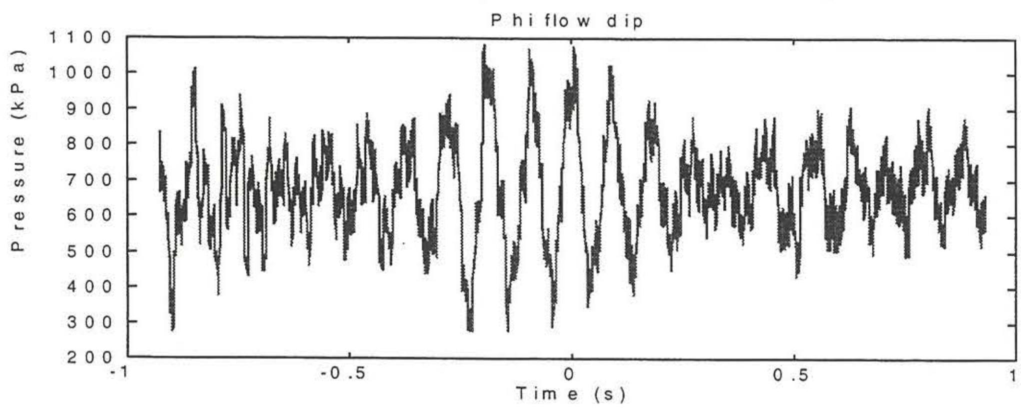


Figure 4b: Plot of Phi, the high-fidelity pressure on the high side of F3F, near a flow dip.

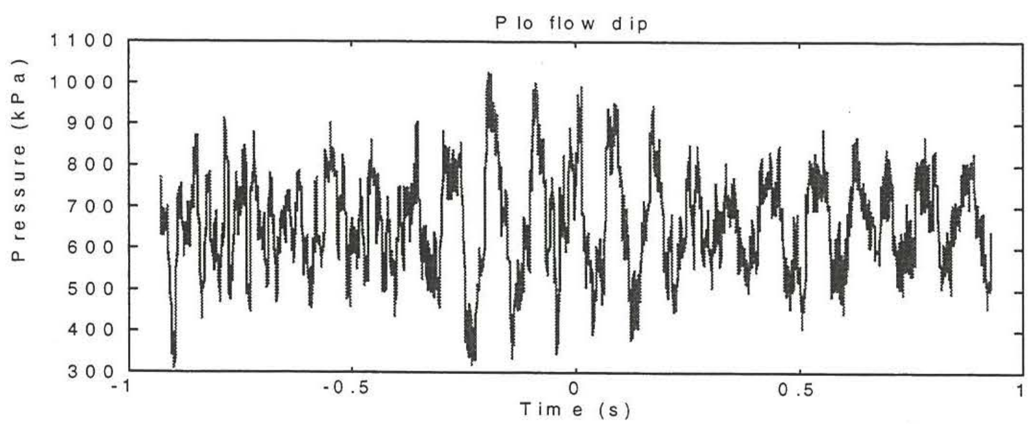


Figure 4c: Plot of Plo, the high-fidelity pressure on the low side of F3F, near a flow dip.

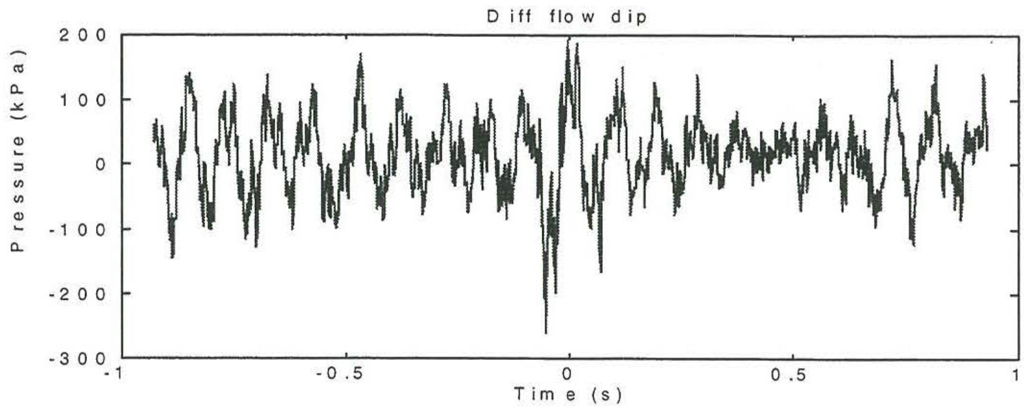


Figure 4d: Plot of Diff (= Phi - Plo) near a flow dip.

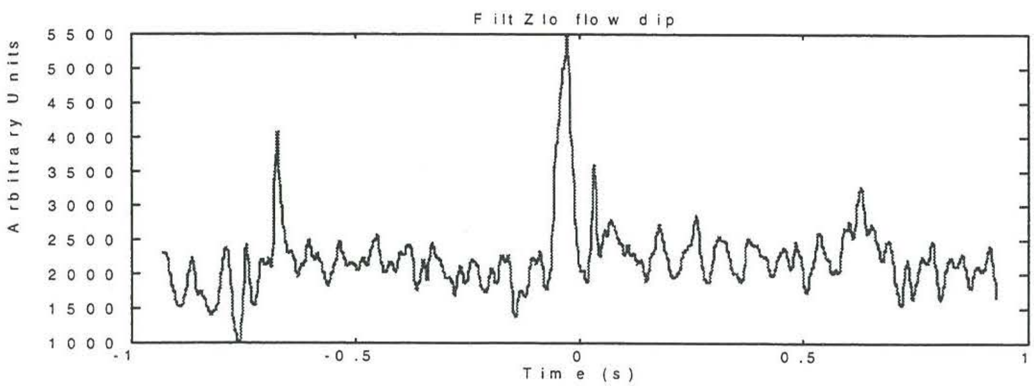


Figure 4e: Plot of FiltZlo, the envelope of the Zlo accelerometer response, near a flow dip.

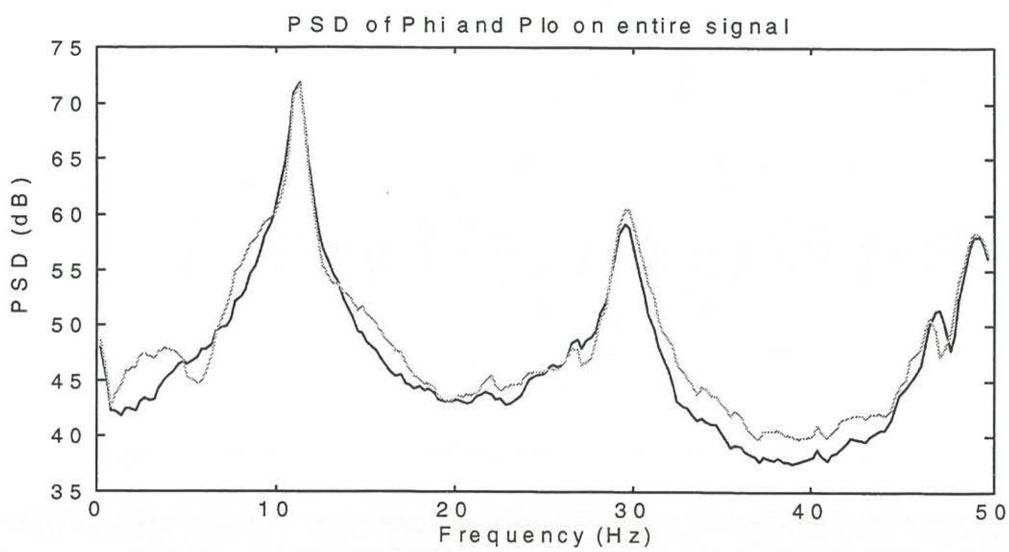


Figure 5: PSDs of Phi (black line) and Plo (grey line).

Transfer functions and coherence functions were calculated for several input-output combinations. The transfer function relating Phi and Diff (Figure 6) can be approximated by equation (2):

$$\frac{\text{Diff}}{\text{Phi}}(s) = k\ e^{-sT} \tag{2}$$

and hence, using equation (1),

$$\frac{\text{Plo}}{\text{Phi}}(s) = 1 - k\ e^{-sT} \tag{3}$$

$$\frac{\text{Diff}}{\text{Plo}}(s) = \frac{k e^{-sT}}{1 - k e^{-sT}} \tag{4}$$

where $s$ = Laplace variable ($s^{-1}$)
$T = 0.18$ s
$k = 0.9$

The Phi-to-Plo transfer function implies that the pressure disturbances initially hit both Phi and Plo almost equally, but that they return after 0.18 s, with the opposite sign and slightly reduced gain, to hit Plo only a second time. This creates a dip in the Plo PSD at about 6 Hz. Several possible theories for this behaviour are presented below.

The Diff-to-F3F transfer function represents the dynamic response of the Rosemount DP cell, and is approximately given by:

$$\frac{\text{F3F}}{\text{Diff}}(s) = \frac{1}{(1+s\tau)^2} \tag{5}$$

where $\tau$ = time constant = 40 ms

The corresponding first-order time constant (63.2% of step) is calculated to be 86 ms. This time constant is considerably smaller than that given in the specifications (200 ms) and as measured using the instrument-air step-response method. A more detailed examination of the response of the DP transmitter to pressure differences is described in a related report [13]. It is suggested in that report that there is a systematic error in the instrument-air step-response measurement method which causes the measured response to be much longer than the true response.

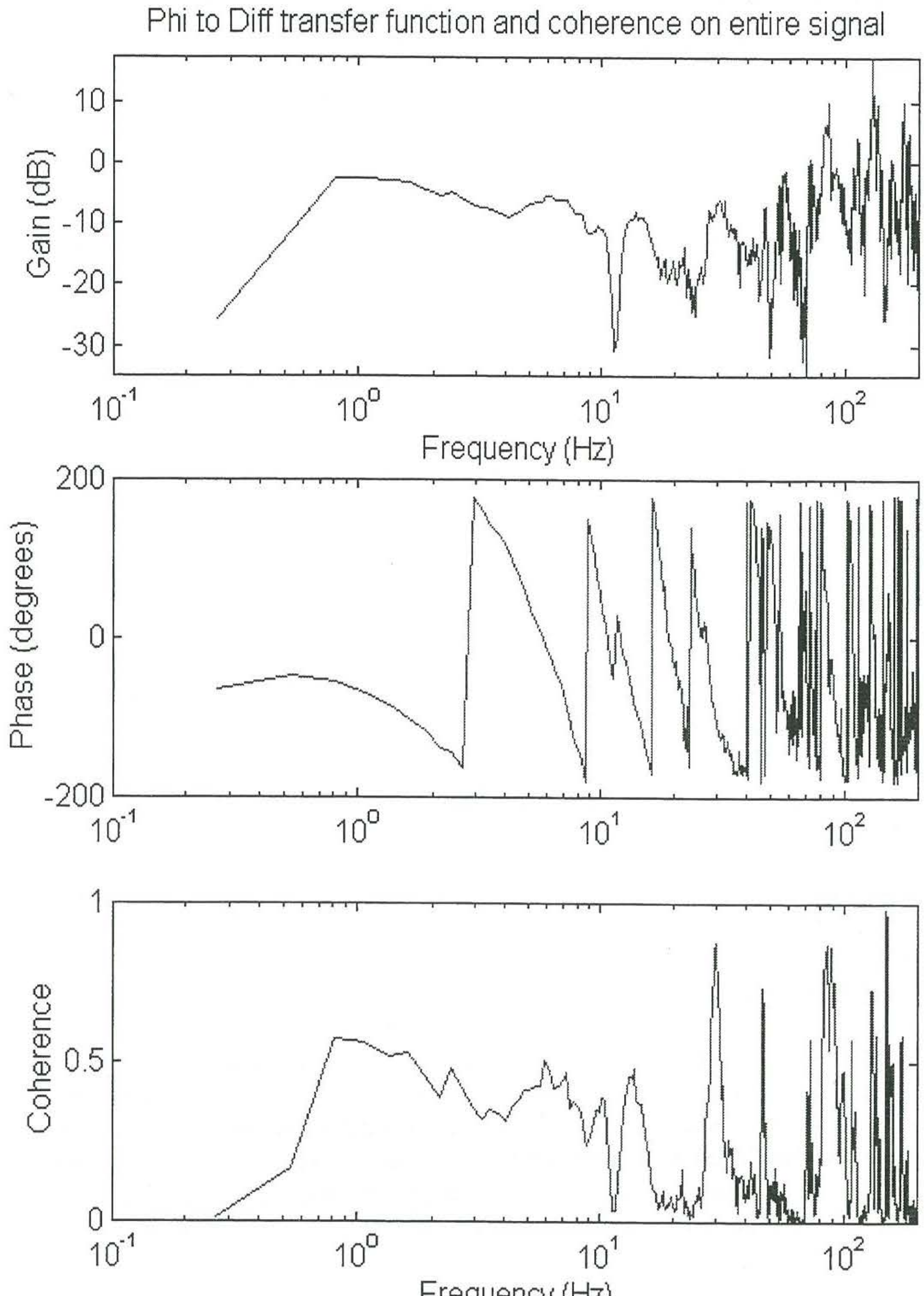


Figure 6: Phi to Diff transfer function.

### 4.2.2 Average Dip Analysis

When looking at a large set of individual dips, it is difficult to distinguish those features that are common and significant from those that are just "noise" (see Figures 4b and 4c). This is especially true in this case, as the noise appears to be at least as large as some of the dip features. Averaging is the common method of reducing noise and hence allowing the "signal" to be more evident. To extract features that are common, an average dip analysis was performed.

The times (indices) associated with the flow dips were identified by finding all points in the F3F signal that represent a local (within ± 80 ms) minimum, and that are also more than a threshold, called the "dip amount", less than the mean value. The conclusions of the average dip analysis, discussed below, of several sets of dips selected using different dip amounts, were found to be not sensitive to the dip amount. Consequently, the -25 kPa dip level (corresponding to a dip below 260 kPa) and its associated 230 flow dips in the 465 s of recorded data were chosen for further analysis and discussion.

After selecting the dips using the above criterion, the data before and after each flow dip point for all signals were then ensemble averaged (Figure 7). By ensemble averaging, signal features that are consistently related to the dip will appear in full strength; signal features that are not consistently related to the dip are attenuated due to the averaging process. Completely random noise is attenuated by a factor of "square root of N", which in our case is about 15 (-24 dB). The dip point in the F3F signal was arbitrarily set to 0 s.

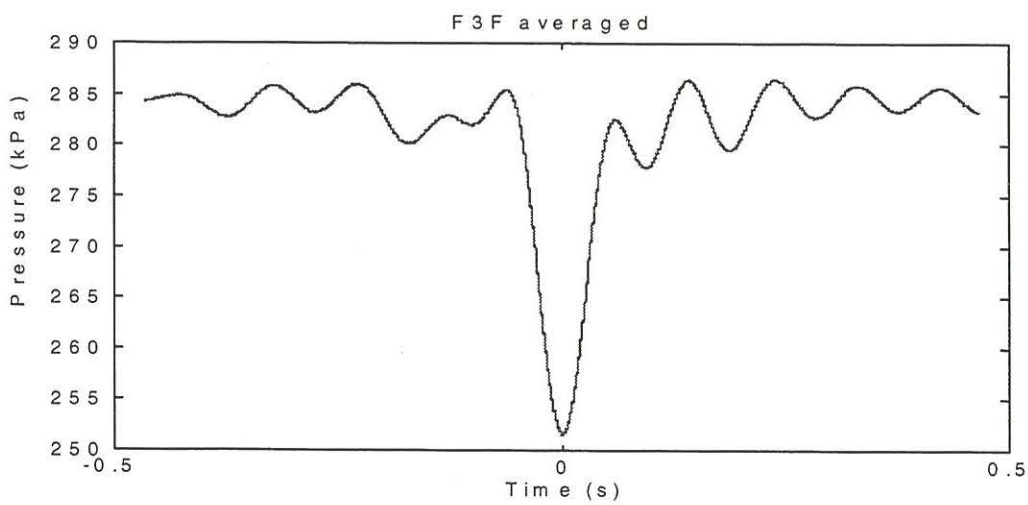


Figure 7a: Average F3F signal expanded about dip.

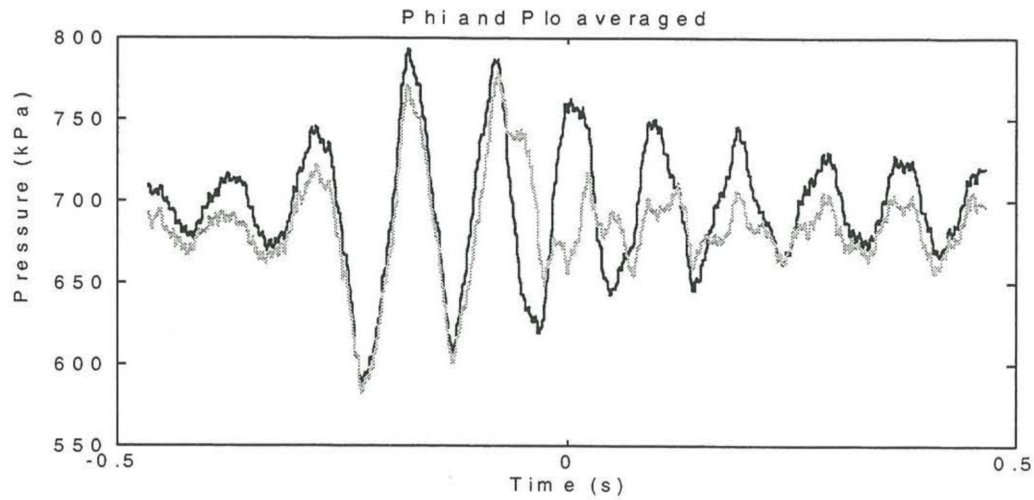


Figure 7b: Average Phi (black line) and Plo (grey line) signal expanded about dip.

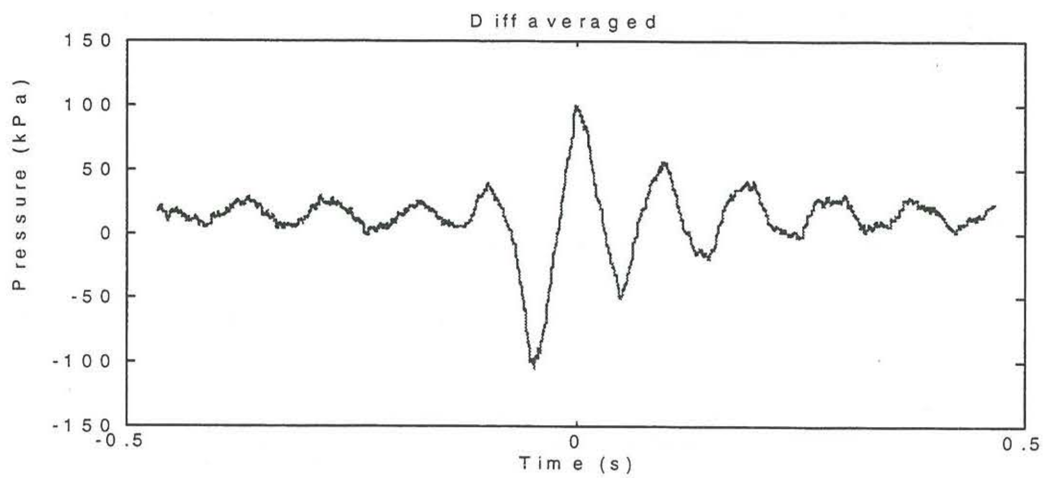


Figure 7c: Average Diff signal expanded about dip.

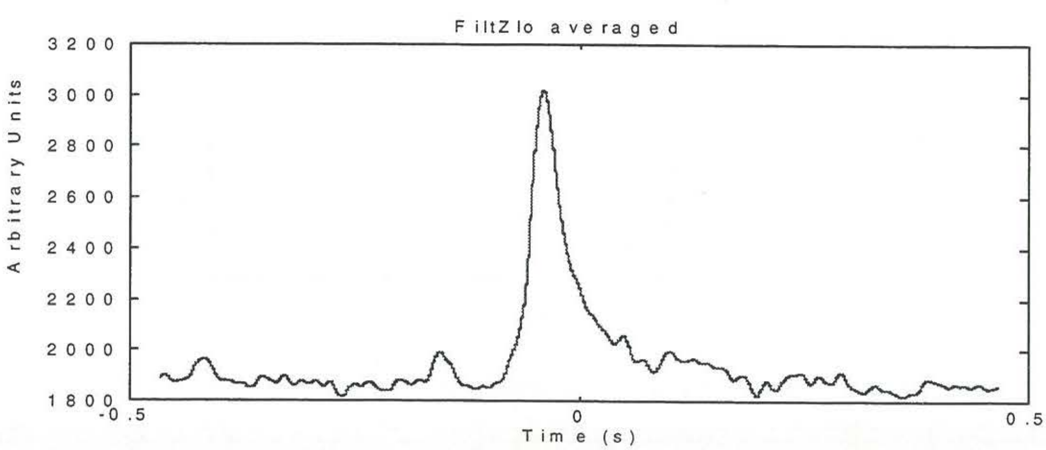


Figure 7d: Average envelope of Zlo (FiltZlo) expanded about dip.

Note that the ensemble-averaged dip in F3F (Figure 7a) is more pronounced than a single dip (Figure 4a) . The Phi and Plo signals (Figure 7b) both have sudden increases in their 10 Hz signal to an amplitude of about ±100 kPa, at t = -0.25 s (i.e., just prior to the flow dip), starting with a negative-going cycle. This increased amplitude of Phi decays in about seven cycles back to the background level. The Plo signal is similar to that of Phi most of the time. However, the increase in the 10 Hz signal for Plo **lasts only two cycles**, and then it drops suddenly back to the background level.

The Diff signal (Figure 8c) has very little noise (± 5 kPa), but just before the dip point at -0.1 s, it exhibits a large, exponentially-decaying, sinusoid with a peak value of -100 kPa. This decaying sinusoid starts on the **third** cycle of the Phi and Plo pressure changes. The first two cycles of Phi and Plo approximately balance, giving little Diff signal, but because the Plo signal drops suddenly, rather than decaying exponentially as the Phi signal does, the Diff signal increases dramatically on the third cycle. The -100 kPa rapid drop in the Diff signal at -0.1 s is then filtered by the response of the slow-acting DP cell to give a -30 kPa flow dip at 0 s.

The disturbances in the Phi, Plo and Diff signals all start with a negative half-cycle. This is consistent with the previous work on DNGS, which showed that the pressure pulses in the DNGS feeder start on the negative half-cycle [11].

The average accelerator envelope signals associated with flow dips have some interesting features. Those associated with the low-side accelerometers (Figure 8d) show a peak **coincident with the lost third cycle of Plo**. This peak is especially large for the high-frequency band (above 250 Hz) signal, while being practically non-existent for the mid-frequency (50 - 250 Hz) band. Those associated with the high-side accelerator also show a similar peak in the high-frequency band component but it is much smaller than that of the low-side accelerometers.

## 5. THEORY

### 5.1 Mismatched Impulse Lines

Based on the Darlington measurements, a theory to explain the relationship between the observed pressure pulses in the inlet header and feeders and how they could cause a flow dip was developed by J. Pascoe of Ontario Hydro [6, 10, 11, 12]. The general sequence of events (discussed in more detail below) is that a pressure pulse originates at the header/feeder junction due to a "burst", travels down the feeder and up the two impulse lines, reaching the two sides of the DP cell almost equally at almost the same time. Due to the resonant properties of the impulse lines, the two impulse line pressure pulses are amplified. If the two impulse lines are mismatched, then the gains are unequal and a DP pulse results.

The details are as follows. The water entering the inlet header from the PHT pumps via the turrets contains vortices. These vortices become detached from the turrets and dissipate in the header. However, there is also a potential second vortex created at the header-feeder junction.

Whether this second vortex is created depends non-linearly on the local conditions which, in turn, are a function of the detached vortices from the turrets. In other words, the turret vortices act like switches for the feeder vortices. The feeder vortex has a characteristic frequency in PNGS of 13.5 Hz.

Thus we have the conditions suitable for a "burst"; this is the term applied when turbulences with different scales (dimensions) interact to give an extraordinarily large effect [14]. Bursts occur randomly in various fields in nature, and cannot be explained simply by Gaussian noise peaks. A burst results in a sudden reduction in pressure as the energy required to create the vortex is taken from the pressure field.

A pair of impulse lines from either side of the orifice plate connect the feeder to the DP cell. Each line is a complex transmission path for pressure waves. It has resonances at a series of frequencies which at PNGS are approximately 10, 30, 50....Hz; these resonances are lightly damped, and thus exhibit high gain (amplification) for pressure pulses. The characteristic resonant frequency of the impulse lines is fairly close to that of the feeder vortex. The damped resonant response of Phi and Plo to a pressure pulse is easily seen in Figure 8b, although the latter only occurs for the first 200 ms.

A small mismatch between the two impulse lines, each of which is amplifying a pressure pulse, would allow the pressure pulse in the feeder to appear as a DP signal (flow dip) at the flow transmitter. Detailed modelling of this system, along with some assumed mismatches, results in the required gain in the frequencies of interest to transform a -120 kPa pressure pulse into a -100 kPa Diff signal and hence a -30 kPa F3F signal, but does not yield anything close to the measured transfer function for Phi to Plo (equation 3). Thus this theory does not quite match all the available data. However, because reasonable mismatches can transform pressure pulses into DP signals of approximately the correct magnitude at the DP cell, this theory should not be rejected outright.

5.2 Other Possible Theories

Other postulated theories for the flow dips follow the above theory up to a point. Bursts and their pressure pulses are the originating cause. The major question is why the response on the low side suddenly damps out after two cycles (Figure 8b). Three possible theories are considered:

(a) interaction with mechanical system

The hydraulic-acoustic resonance within the impulse lines causes mechanical vibration of the impulse tubing. If one of these tubes is only loosely supported, it may hit something, changing the mechanical vibrations, and initiating a new set of mechanical resonances. The energy that was originally mostly hydraulic-acoustic can be transformed into high-frequency mechanical activity, which has much higher damping (as viewed in seconds, not in cycles), thus dissipating the energy. The net effect is to damp out the pressure resonance. This transfer of energy will be dependent on the details of the impulse lines, including their supports and clamps.

The problems with this theory are:

- statistically, loose supports are just as likely on the high side as on the low side, leading to both flow dips and peaks, which is not consistent with the fact that only flow dips, not flow peaks, have been seen.
- although flow dips and mechanical activity normally occur together, there are a few instances of one or the other of them occurring separately.

Thus the theory is plausible, but is not completely supported by the available data, and there is some data to contradict it.

(b) effect of vortex remnants

The temporary vortex at the header/feeder junction, which creates the original pressure pulse, eventually travels down the feeder as well, dissipating as it goes. Although we have the required length of straight diameters as specified in the ISO standard [2] for the 0.5% increased uncertainty, there may still be a remnant of the vortex left at the orifice. Given the fluid velocity in the feeder, it would take about 140 ms to reach the orifice plate, which corresponds fairly well to the 180 ms given as a parameter T in equations (2, 3 and 4). One might think that, as the vortex remnant moves through the orifice plate, the pressure drop would initially increase, and then decrease again to its normal level. The problem with this theory is that this should produce a pressure drop on the low-pressure side, not a pressure rise as observed.

(c) non-linear effects

Discontinuities in the flow path can cause non-linearities in the pressure-flow relationship. For instance, a sudden expansion or contraction will have a different pressure drop in one direction than in the other direction for the same absolute flow. Valves, even open valves, are a similar cause of non-linearity. Non-linearities act partially like diodes to flow. There are a number of hydraulic non-linearities in the impulse lines. These include the impulse line/feeder junctions, the three-way manifold valves, and, on the high side, the Hoke valve. It is conceivable that one or more of these non-linearities might act to restrict the flow sufficiently in one direction to damp out the third cycle. The problem with this theory is that there is no evidence of these non-linearities during the first one and three quarter cycles.

## 7. CONCLUSIONS

The conclusions of this research are that flow dips are not caused by a change in flow but are an artefact of pressure pulses. In particular:

(1) The flow dips are definitely not caused by either the DP cell itself or anything electrical. At the time a flow dip occurs, there is a true differential pressure change of a very large magnitude (-100 kPa typical, -500 kPa maximum) across the DP cell.
(2) The flow in the PHT quadrant in general is definitely not changing significantly during a flow dip. The flow in the individual feeder in question, as a whole, also cannot be changing to the extent indicated by the Diff signal, as measured with the temporarily-installed pressures cells .
(3) The theory for flow dips originally developed at DNGS has been mostly supported by these PNGS measurements. Pressure pulses originating at the header/feeder junction are still

believed to be the root cause of the flow dip phenomena. However, the precise mechanism by which a pressure pulse is transformed into a flow dip has not yet been determined. Four possible theories have been postulated:

- mismatched impulse lines (the original DNGS theory),
- energy transfer from hydraulic-acoustic to mechanical modes, and
- remnants of vortices passing through the orifice plate,
- non-linear effects at discontinuities.

None of these theories fully explain all the observations. Additional theories are also possible.

(4) The high- and low-side impulse lines from the orifice plates exhibit very large pressure variations (±400 kPa typical). Similar variations in pressure are not evident on any of the other impulse lines connected to the PHT system; the FINCH DP cell impulse lines have ±150 kPa typical.

(5) These large pressure variations result in vibrations and other mechanical motions of the impulse lines. Some high-frequency mechanical motion is normally associated with the flow dips; it is not clear whether this is a cause or an effect.

(6) The transfer function of the Rosemount model 1152 DP cells to differential pressure changes has been accurately measured. The time constant of the PNGS unit 6 F3F DP cell alone is approximately 86 ms. A detailed report on this topic has been issued [13], and is the subject of a related paper.

## 8. RECOMMENDATIONS

There are two sets of recommendations based on the findings that flow dips are not caused by a change in flow, but are an artefact of pressure pulses. The first set of recommendations is for existing plants in which it is difficult to replace or modify equipment, and the second set is for new plants, in which many changes are feasible.

### 8.1 Recommendations for PNGS and Other Existing Plants

(1) Increase the damping of the LGF DP cells. The increased damping (time constant) must be consistent with the safety analysis.

(2) Measure the time constant using a more accurate method, based on true DP. The current method of measuring the time constant is too conservative. Some possible other methods are given in [15].

(3) Inspect the impulse lines to check for damage caused by fretting. Replace/repair any defective impulse lines.

(4) Inspect the supports and clamps used to hold the impulse lines for long unsupported runs and/or loose clamps. Install additional and/or tighten existing clamps as required.

## 8.2 Suggestions for New CANDUs

There are a number of changes suggested below that could be implemented in new CANDU designs. The objective of most of these changes is to prevent the formation of pressure pulses in the first place and/or to inhibit their transmission through to the DP cells. However, because the root causes postulated are as yet unproven theories, some of the suggestions may or may not be effective. A further R&D program should be initiated to discover the exact mechanism of pressure pulse transformation into flow dips.

(1) The feeder selected for the LGF measurement should connect to the header as far as possible from the pump turrets.
(2) The shape of the header/feeder junction geometry should be modified to minimize the formation of vortices.
(3) The use of venturis and/or flow nozzles should be considered in place of orifice plates. There is no evidence of flow dips on the FINCH channels, which use venturis.
(4) Two pressure-sensing taps connected in parallel should be used for both high- and low-pressure connections, to minimize differential pressure noise, as recommended in the instrumentation handbook [16].
(5) The taps should be aligned perpendicular to the plane of the nearest upstream bend.
(6) The orifice plate and tap holes should be manufactured strictly according to the ISO standard in all respects, unless there is positive evidence that deviations improve performance.
(7) The channels selected should have a header/feeder junction vortex frequency that is significantly different from the resonant frequency of the impulse by selecting different channels or by changing the diameter of the selected channels.
(8) The impulse lines should be adequately clamped over their whole length.
(9) The impulse lines on the two sides of the DP cell should be very closely matched.
(10) The safety analysis should be performed with assumed DP cell time constants of at least 500 ms to allow the station to increase the damping as required.

# 9. ACKNOWLEDGMENTS

The author would like to thank Martin Tulett, Don Williams, Sonya von Svoboda and Oszvald Glockler of Ontario Hydro Pickering NGS for their organization of, and participation in, the experiments.

The work reported in this paper was funded by the CANDU Owners Group (COG) R&D Program:

Working Party No. 16 WPIR No. 1636

## 10. REFERENCES


[1] O. Glockler, "Pressure and Flow Noise Measurements in PNGS Unit 6", Ontario Hydro report PB-IR-63700-8.

[2] "Measurement of Fluid Flow by means of Orifice Plates, Nozzles and Venturi Tubes Inserted in Circular Cross-section Conduits Running Full", ISO Standard 5167, 1980.

[3] Ontario Hydro, "Pickering Generating Station B Safety Report", Vol II Table 13.3.3.2-3, rev Jan 1985.

[4] A. Ling, "Pickering NGS-B Unit 6 SDS1 Heat Transport Low Flow Trip Time Constant", AECB memo to P.R. Charlebois, 1994 February 23.

[5] C. Olive, personal communication, 1987 May 20.

[6] J. Pascoe, personal communication, 1992 December 16.

[7] Y.C. Wan, personal communication, 1994 June 17.

[8] G.Y. Wong, J.M. Cuttler and R.S. Kohli, "Shutdown System Number 1: Part 4 - Process Trip Parameters", PNGS B Design Manual NK30-63720.4, rev 1985 November.

[9] O. Glockler, personal communication, 1995-05-21.

[10] D. Martin and J. Pascoe, "Final Report on the Darlington NGS Unit 3 Test Program", Ontario Hydro report no. 931022, 1993 October 01.

[11] J. Pascoe, personal communication, 1993 February 09.

[12] J. Pascoe, personal communication, 1992 October 28.

[13] Y. Gao, H. W. Hinds and P. D. Tonner, "An Accurate Measurement of the Rosemount 1152 Differential Pressure-Cell Response Time", COG-95-592, 1996 June.

[14] E. Mollo-Christensen, "Intermittency in Large-Scale Turbulent Flows", Annual Review of Fluid Mechanics, p 101, 1973.

[15] Instrument Society of America, "Response time Testing of Nuclear Safety-Related Instrument channels in Nuclear Power Plants", ISA standard S67.06, 1984.

[16] B.G. Liptak (ed.), "Process Measurement and Analysis", Instrument Engineers' Handbook, 3rd edition p154, Chilton Book Co., 1995.